

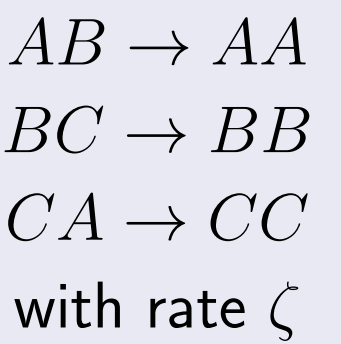
Figure 1: (a) Cyclic dominance in *E. coli* (b) Spiral pattern formation in the Belousov-Zhabotinsky reaction (source)

A number of systems in the fields of ecology, epidemiology, and chemistry follow a paradigm of cyclic dominance (e.g. certain subspecies of Lizards in California [1], experiments on cyclically competing *E. coli* bacteria [2], and Belousov-Zhabotinsky reaction). The formation of noise-induced and -stabilized spiral patterns in this class of system is captured by the spatially-extended May-Leonard (ML) model. The formation of these spirals is in stark contrast to the species clustering seen in the Rock-Paper-Scissors (RPS) model.

The RPS Model

The RPS Model is defined by the following binary reactions:

- Replacement Reaction:



- Pair Swap / Diffusion Reaction:

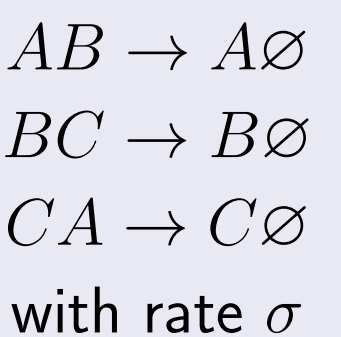


where $X, Y \in \{A, B, C, \emptyset\}$ with rate ϵ_r

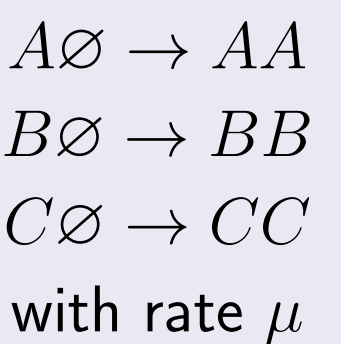
The May-Leonard Model

The ML Model is defined by the following binary reactions:

- Predation Reaction:



- Reproduction Reaction:



- Pair Swap / Diffusion Reaction:



$X, Y \in \{A, B, C, \emptyset\}$ with rate ϵ_m

Simulation

We define x to be the vertical (short) axis and y to be the horizontal (long) axis. A lattice of size $L_x \times L_y$ is then initialized with each cell being assigned a random species with probability $p(A) = p(B) = p(C) = \rho_0/3$ (where ρ_0 is the initial net particle density). We limit each lattice point to contain at most one particle. The lattice is given a toroidal topology (i.e. $x = 0$ is equivalent to $x = L_x$ and likewise for y). The simulation then proceeds according to the following algorithm:

1. A random coordinate (x, y) is selected from a uniform distribution and time is advanced by $\delta t = P^{-1}$ (where $P = L_x \times L_y$).
2. If that lattice point is not empty, then a nearest neighbor is chosen at random. If the cell is empty, the simulation returns to step 1.
3. One of the possible reactions (according to whether the lattice point is governed by the ML or RPS model) is selected at random, and executed if possible. The simulation returns to step 1.

In cases where there are both RPS and ML lattice points, all lattice points in the range $0 \leq y < d_i$ are governed by the RPS model and all remaining lattice points are governed by the ML model.

Boundary Effects in Stochastic Cyclic Competition Models on a Two-Dimensional Lattice

M. Lazarus Arnau, Shannon Serrao, Uwe C. Täuber

Department of Physics (MC 0435) and Center for Soft Matter and Biological Physics
Virginia Tech, Blacksburg, Virginia 24061

July 26, 2018

We study noise-induced and -stabilized spatial patterns in two distinct stochastic population model variants for cyclic competition of three species, namely the Rock-Paper-Scissors (RPS) and the May-Leonard (ML) models.

In two dimensions, it is well established that the ML model can display (quasi-)stable spiral structures, in contrast to simple species clustering in the RPS system. Our ultimate goal is to impose control over such competing structures in systems where both RPS and ML reactions are implemented. To this end, we have employed Monte Carlo computer simulations to investigate how changing the microscopic rules in a subsection of a two-dimensional lattice influences the macroscopic behavior in the rest of the lattice. Specifically, we implement the ML reaction scheme on a torus, except on a ring-shaped patch, which is set to follow the cyclic Lotka-Volterra predation rules of the RPS model. There, we observe a marked disruption of the usual spiral patterns in the form of plane waves emanating from the RPS region, up to a characteristic distance that is set by the diffusion rate in the RPS patch. Furthermore, the overall population density drops considerably in the vicinity of the interface between both regions.

Normal Pattern Formation

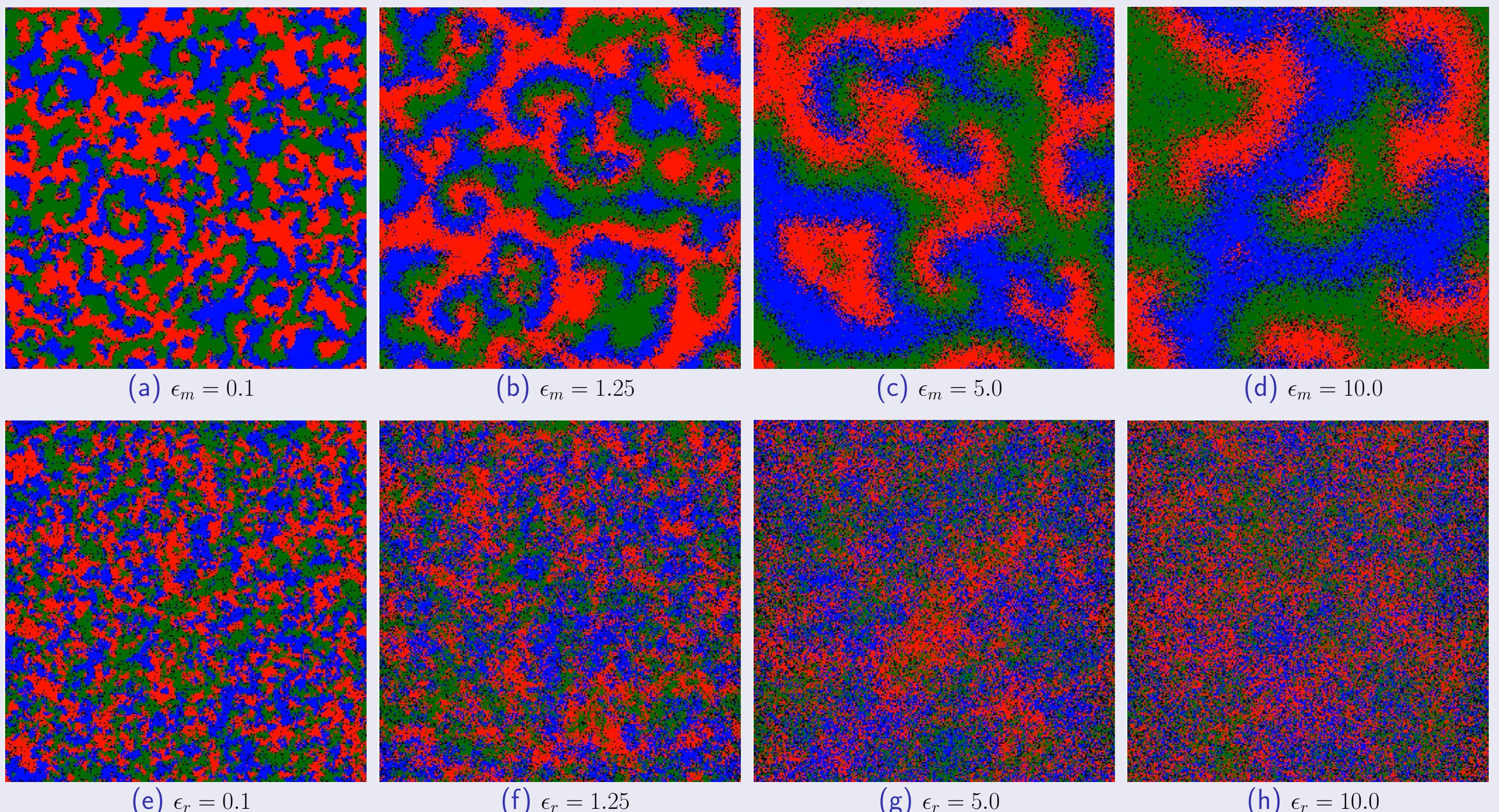


Figure 2: Steady State snapshots. All lattices have $L_x = L_y = 256$: (a)-(d) Typical ML pattern formation. $\sigma = \sigma = \mu = 1.0$ (e)-(h) Typical RPS pattern formation. $\zeta = 1.0$

Plane Wave Formation

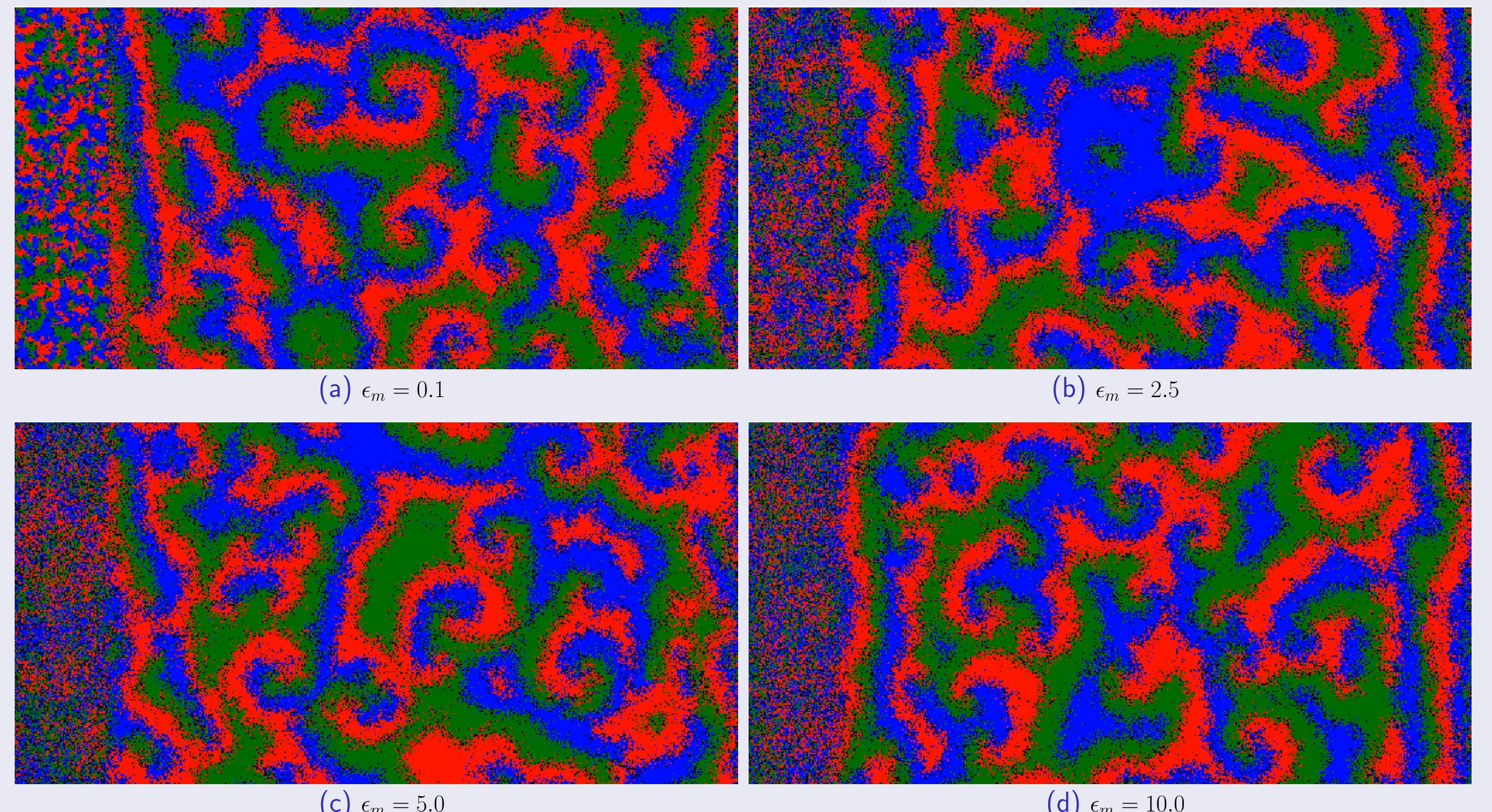


Figure 3: Steady state snapshots. Plane wave formation in 256×512 lattices. In all cases $\epsilon_m = 2.5$, $\sigma = \mu = 1.0$, $\zeta = 1.0$. The interface is placed at $y = 64$

Characteristic Dynamics of the ML Model

The following values were derived analytically by Reichenbach, et. al. [3]

Diffusion Constant: $D = \epsilon_m d^{-1} N^{-2/d}$

where d is the number of spatial dimensions and N is the size of the lattice.

Constants: $c_1 = \frac{1}{23\mu + \sigma}$, $c_3 = \frac{\sqrt{3}(18\mu + 11\sigma)}{48\mu + 11\sigma}$

Spreading Velocity: $v^* = 2\sqrt{c_1 D}$

Wavelength: $\lambda = \frac{2\pi c_3 \sqrt{D}}{\sqrt{c_1} \left(1 - \sqrt{1 + c_3^2}\right)}$

We use these values to contextualize our measurements in the next section. For the cases shown below we use $d = 2$ and $N = W \times H = 2^{17}$, $\sigma = \mu = \zeta = 1.0$, and $\epsilon_m = 2.5$. This yields theoretical values of $D \approx 9.5 \times 10^{-6}$, $v^* \approx 0.00218$, and $\lambda \approx 0.18$

Plane Wave Behavior:

| ϵ_m | d_p | v | $2\tau v$ |
|--------------|-------|----------|-----------|
| 0.01 | 0.119 | 0.000198 | 0.00178 |
| 2.5 | 0.168 | 0.000206 | 0.00185 |
| 5.0 | 0.168 | 0.000192 | 0.00173 |
| 10.0 | 0.129 | 0.000194 | 0.00175 |

Using plots of density measured parallel to the interface, we visually estimate the permeation distance (d_p) and front velocity (v^{num}) of the plane-waves. We also rescale velocity by 2τ (where $\tau = \epsilon_m + \sigma + \mu$) in order to account for differences in how time scaling is handled in [3]. Note that, in source, numerical results for spreading velocity deviate from their analytical result by $\approx 10\%$. We thus see that, unsurprisingly, plane waves travel at approximately the characteristic spreading velocity of the system. We also find that d_p is on the scale of the characteristic wavelength, reaching a maximum when ϵ_r is close to ϵ_m .

Interface Density Effects

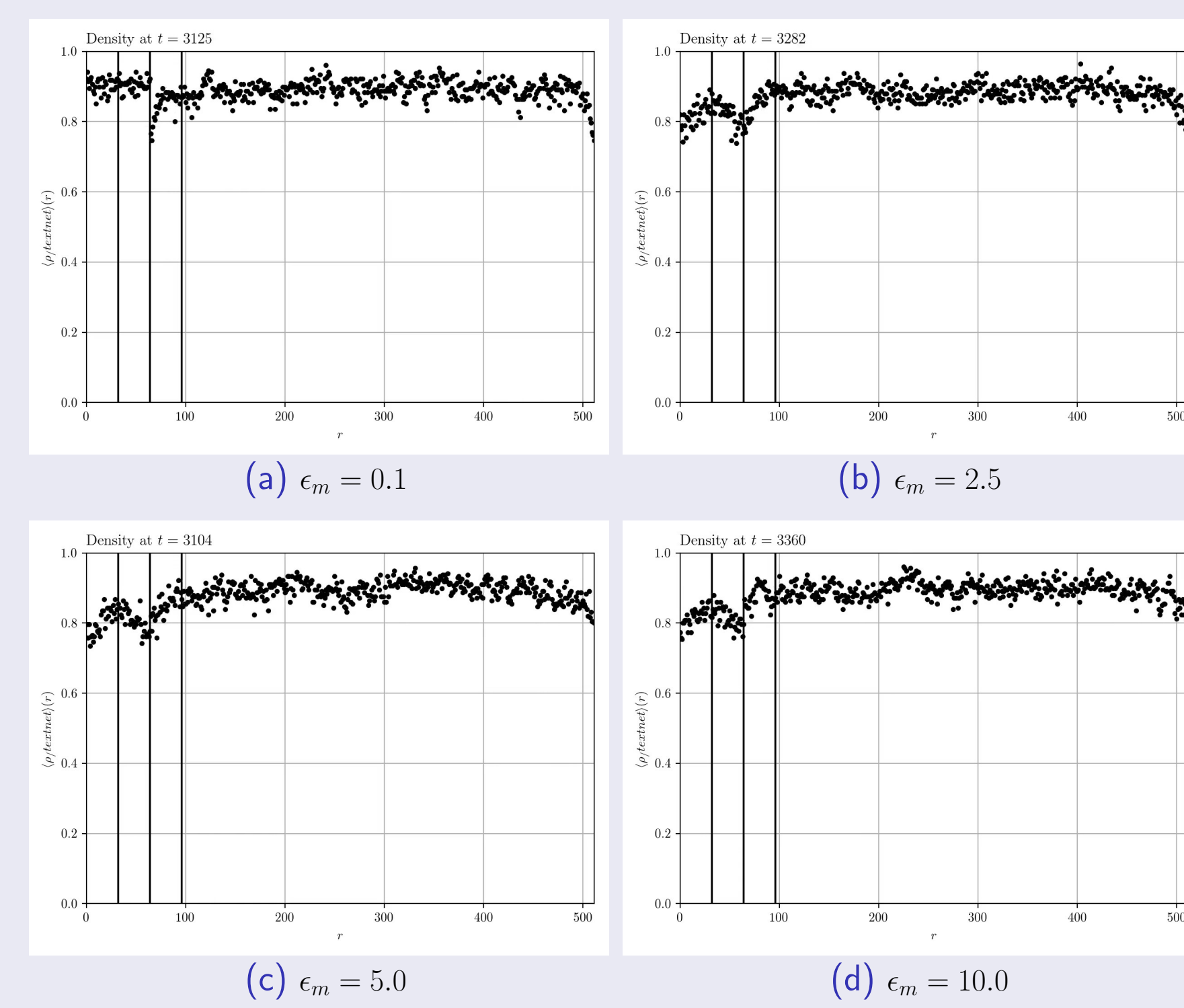


Figure 4: Plane wave formation in 256×512 lattices. In all cases $\epsilon_m = 2.5$, $\sigma = \mu = 1.0$, $\zeta = 1.0$. The interface is placed at $y = 64$

One surprising result produced by our simulations is a notable drop in net particle density in the immediate vicinity of the interface (the center black line in figure 4). We find that the greatest drop in density occurs on the side of the boundary with the higher diffusion rate.

Future Work

- Visual measurements of the plane wave behavior severely limits both the volume of and accuracy with which we can collect data. We will use FFTs to analyze space-time density plots.
- The exact cause of the drop in net density near the interface is not yet apparent, and as such this presents us with a clear next step.

References

- [1] B. Sinervo and C. Lively, "The rock-paper-scissors game and the evolution of alternative male strategies," vol. 380, pp. 240–243, 03 1996.
- [2] B. Kerr, M. Riley, M. Feldman, and B. Bohannan, "Local dispersal promotes biodiversity in a real-life game of rock-paper-scissors," vol. 418, pp. 171–174, 01 2002.
- [3] T. Reichenbach, M. Mobilia, and E. Frey, "Self-organization of mobile populations in cyclic competition," vol. 254, pp. 368–383, 09 2008.

Acknowledgement



Research was sponsored by the U.S. Army Research Office and was accomplished under Grant Number W911NF-17-1-0156.